'89 KACC 1989. 10. 27~28

Analysis of Singularity and Redundancy Control for Robot-Positioner System

°E.S.Jeon* J.W.Chang** J.E.Oh* S.H.Yum*

* HanYang Univ.,Dept. of Prec. Mech. Eng.

** GoldStar Telecommunication Co.,LTD

Recently industrial robots are often used together with positioners to enhance the system performance for arc welding. In this paper, the redundaney control method is proposed for the robot-positioner system which is modeled as one kinematic model of 7 degrees of freedom. Also, the manipulability measure based on the Jocobian matrix is utilized to visualize the distribution of manipulability in a given section of the working space. An algorithm for the manipulability maximazation in a given task is developed and applied to the robot and positioner system. The simulation results are given in the case of straight line following.

1. INTRODUCTION

Recently, as the productivity and the better quality are highly demanded in the industry, the automated machinery including the industrial robots is used in factories. To increse the performance and the flexibility of the industrial robot, more degrees of freedom are added to the robot or it is used in combination with a positioner in the industry. Especially in the poor working environment such as welding operation, the use of a positioner is very helpful. For this purpose, Khosla, et al (1986) combined the cartesian coordinate robot with a positioner system (called R-P system in this paper) for the seam tracking and modeled the whole system as the robot with six degrees of freedom. Also, by Jeon, et al(1986) the robot system control with one kinematic model was suggested.

In the trajectory control of a robot, however, the nonlinear relation between cartesian space and joint space gives rise to problems of singularity. The performance index evaluation related with a robot's structure was suggested to be the multiplication of singular values by Yoshikawa (1984) and Uchiyama, et al (1984). Also, the performance index and its gaphic representation of 2-joint robotic manipulator were reasearched by Homsup and Anderson (1986). The industrial robots, however, need more degree of freedom for obstacle avoidance and efficient operation.

In this paper, a 5-degree articulated robot and a 2- degree positioner are modelled and analyzed as one kinematic system. Its redundancy control and validity are to be investigated. For this purpose, the inverse kinematic solution of the R-P system with the positioner tilting angle fixed is found and the singularity of Jacobian is analyzed. To investigate the effect of redundancy upon the R-P system manipulability, the manipulability measure is calculated with the inverse kinematic solution. The joint angle with high manipulability is decided based on manipulability measure distribution graph. The redundant angles decided above are compared with the angles based on the inverse kinematic solution only to investigate whether the later satisfies high manipulability.

2. THE KINEMATIC ANALYSIS OF A R-P SYSTEM

The R-P system is composed of a 5-degree articulate robot and a 2-degree positioner and its coordinate is decided as follows. As the work is carried out on the positioner in this R-P system, the refernce coordinate is on the positioner. For the robot and the positioner to be one kinematic model, the joint angles are denoted by Denavit-Hartenberg method. As explained in Table 1 and Fig.1, the coordinate transformation matrices are found as follows.

Table 1 Link parameters of R-P system

Link	θ_i	α_i	a_i	d_i
1	θ_1	90°	0	−3.03
2	θ_2	−90°	−11.80	0
3	θ_3	−90°	0	5.04
4	$\theta_4+90°$	0°	9.00	0
5	$\theta_5-90°$	0°	9.00	0
6	θ_6	−90°	0.35	0
7	θ_7	0°	0	6.30

(unit : inch)

$$A_1=\begin{bmatrix} c_1 & 0 & s_1 & 0 \\ s_1 & 0 & -c_1 & 0 \\ 0 & 1 & 0 & d_1 \\ 0 & 0 & 0 & 1 \end{bmatrix} \quad (1)$$

$$A_2=\begin{bmatrix} c_2 & 0 & -s_2 & a_2c_2 \\ s_2 & 0 & c_2 & a_2s_2 \\ 0 & -1 & 0 & 0 \\ 0 & 0 & 0 & 1 \end{bmatrix} \quad (2)$$

$$A_3=\begin{bmatrix} c_3 & 0 & -s_3 & 0 \\ s_3 & 0 & c_3 & 0 \\ 0 & -1 & 0 & d_3 \\ 0 & 0 & 0 & 1 \end{bmatrix} \quad (3)$$

$$A_4=\begin{bmatrix} s_4 & c_4 & 0 & a_4s_4 \\ -c_4 & s_4 & 0 & -a_4c_4 \\ 0 & 0 & 1 & 0 \\ 0 & 0 & 0 & 1 \end{bmatrix} \quad (4)$$

$$A_5=\begin{bmatrix} -s_5 & -c_5 & 0 & -a_5s_5 \\ c_5 & -s_5 & 0 & a_5c_5 \\ 0 & 0 & 1 & 0 \\ 0 & 0 & 0 & 1 \end{bmatrix} \quad (5)$$

$$A_6=\begin{bmatrix} c_6 & 0 & -s_6 & a_6c_6 \\ s_6 & 0 & c_6 & a_6s_6 \\ 0 & -1 & 0 & 0 \\ 0 & 0 & 0 & 1 \end{bmatrix} \quad (6)$$

$$A_7=\begin{bmatrix} c_7 & -s_7 & 0 & 0 \\ s_7 & c_7 & 0 & 0 \\ 0 & 0 & 1 & d_7 \\ 0 & 0 & 0 & 1 \end{bmatrix} \quad (7)$$

Therfore, the transformation matrix of the R-P system is given as follows and each components are shown in Table 2.

$$T_7 = A_1A_2A_3A_4A_5A_6A_7 \tag{8}$$

Table 2 Direct kinematic solution for R-P system

$$\begin{bmatrix} c_1(c_2r_{11}-s_2r_{31})-s_1r_{21} & c_1(c_2r_{12}-s_2r_{32})-s_1r_{22} & 0 & c_1(c_2r_{14}-s_2r_{34}+c_2a_3)-s_1r_{24} \\ s_1(c_2r_{11}-s_2r_{31})-c_1r_{21} & s_1(c_2r_{12}-s_2r_{32})+c_1r_{22} & 0 & s_1(c_2r_{14}-s_2r_{34}+c_2a_3)+c_1r_{24} \\ s_2r_{11}+c_2r_{31} & s_2r_{12}+c_2r_{32} & 0 & s_2r_{13}+c_2r_{33} \\ 0 & 0 & 0 & 1 \end{bmatrix}$$

$$\begin{bmatrix} c_1(c_2r_{14}-s_2r_{34}+c_2a_3)-s_1r_{24} \\ s_1(c_2r_{14}-s_2r_{34}+c_2a_3)+c_1r_{24} \\ s_2(r_{14}+a_3)+c_2r_{34}+d_1 \\ 1 \end{bmatrix}$$

To find the inverse kinematic solution, from equation (8),

$$(A_2)^{-1}(A_1)^{-1}T_7 = A_3A_4A_5A_6A_7 \tag{9}$$

left side of equation (9) is

$$\begin{bmatrix} c_2(c_1n_x+s_1n_y)+s_2n_z & c_2(c_1o_x+s_1o_y)+s_2o_z & c_2(c_1a_x+s_1a_y)+s_2a_z & c_2(c_1p_x+s_1p_y)+s_2(p_z-d_1)-a_2 \\ -s_1n_x+c_1n_y & -s_1o_x+c_1o_y & -s_1a_x+c_1a_y & -s_1p_x+c_1p_y \\ -s_2(c_1n_x+s_1n_y)+c_2n_z & -s_2(c_1o_x+s_1o_y)+c_2o_z & -s_2(c_1a_x+s_1a_y)+c_2a_z & -s_2(c_1p_x+s_1p_y)+c_2(p_z-d_1) \\ 0 & 0 & 0 & 1 \end{bmatrix} \tag{10}$$

and right side is

$$\begin{bmatrix} r_{11} & r_{12} & r_{13} & r_{14} \\ \cdot & \cdot & r_{23} & r_{24} \\ r_{31} & r_{32} & r_{33} & \cdot \\ 0 & 0 & 0 & 1 \end{bmatrix} \tag{11}$$

Now we assume the arbitrary tilting angle of the positioner.

$$\theta_2 = C \tag{12}$$

$$\frac{r_{23}}{r_{13}} = \frac{r_{24}}{r_{14}} \tag{13}$$

Rewrite the eqution (13), we can find as follows;

$$c_1\{s_2(a_2p_y-a_y(p_z-d_1))+a_2a_y\}+s_1\{s_2(a_x(p_z-d_1)-a_2p_x)-a_2a_x\}=c_2(p_xa_y-p_ya_x) \tag{14}$$

Substituting eqution (14) by the trigonometry,

$$c_1A+s_1B=K \tag{15}$$

Where

$$A = s_2(a_2p_y-a_y(p_z-d_1))+a_2a_y$$
$$B = s_2(a_x(p_z-d_1)-a_2p_x)-a_2a_x$$
$$K = c_2(p_xa_y-p_ya_x)$$

When we put A=Rcosϕ, B=Rsinϕ, Eq.(15) becomes;

$$s_1c_\phi+c_1s_\phi=\frac{K}{R}$$

$$s(\theta_1+\phi)=\frac{K}{R} \tag{16}$$

where $R=\sqrt{A^2+B^2}$, $\phi=\tan^{-1}\left(\frac{B}{A}\right)$

then $$c(\theta_1+\phi)=\sqrt{1-\frac{K^2}{R^2}} \tag{17}$$

Therefore,

$$\theta_1=-\tan^{-1}\left(\frac{B}{A}\right)+\tan^{-1}\left(\frac{K}{\sqrt{A^2+B^2-K^2}}\right) \tag{18}$$

For calculating angle $\theta 3$, we set

$$\frac{r_{24}}{r_{14}}=\frac{s_2}{c_2} \tag{19}$$

$$\theta_3=\tan^{-1}\left[\frac{-s_1p_x+c_1p_y}{c_2(c_1p_x+s_1p_y)+s_2(p_z-d_1)-a_2}\right] \tag{20}$$

Calculating $\theta 1$ as the same way, we can be shown as Table 3.

Table 3 Inverse kinematic solution for R-P system

Joint coordinate	Analytical expression
θ_1	$-\tan^{-1}(\frac{B}{A})+\tan^{-1}(\frac{K}{\sqrt{A^2+B^2-K^2}})$
θ_2	Arbitary Constant
θ_3	$\tan^{-1}\left[\frac{-s_1p_x+c_1p_y}{c_2(c_1p_x+s_1p_y)+s_2(p_z-d_1)-a_2}\right]$
θ_4	$\tan^{-1}\left[\frac{\alpha a_5c_5+\beta(a_4-a_5s_5)}{\beta a_5c_5-\alpha(a_4-a_5s_5)}\right]$
θ_5	$\sin^{-1}\left[\frac{\alpha^2+\beta^2-a_4^2-a_5^2}{2a_4a_5}\right]$
θ_6	$\theta_{456}-\theta_4-\theta_5$
θ_7	$\tan^{-1}\left[\frac{-s_2(c_1o_x+s_1o_y)+c_2o_z}{-s_2(c_1n_x+s_1n_y)+c_2n_z}\right]$

3. THE PERFORMANCE EVALUATION OF A R-P SYSTEM

3-1. The Performance Measure for Manipulability Evaluation

Let (i=1,2, ... ,n) be the joint variables of a robot a manipulator with n degree of freedom and suppose that we can describe the desired task, and X with the number of m variables. Then, the relation between θ and X is given as;

$$X = f(\theta) \tag{21}$$

where : joint space vector
: cartesian space vector

The X is called as manuplability variable to explane the work of robot.

Because eq.(21) is nonlinear equation, it is rewritten n by linearization as follows:

$$dX = J(\theta)d\theta \tag{22}$$

where dX : differential change of X
$d\theta$: differential change of θ
$J(\theta) = \partial f(\theta)/\partial\theta$: Jacobian matrix

Yoshikawa and Uchiyama explained the manipulability measure in such a way that X or dX can be decised by θ or $d\theta$ and suggested the use of Jacobian matrix toevaluate it (Yoshikawa, 1984 ; Uchiyama et al, 1984).

This manipulability of a robot is quantified as the manipulability measure. The manipulability measure is defined as follows :

(i) m = n

$$\omega(\theta)=|\det J(\theta)| \tag{23}$$

(ii) m < n

$$\omega(\theta)=\sqrt{\det(J(\theta)J^T(\theta))} \tag{24}$$

When rank $J(\theta)$ = m, the redundant degree of freedom for a robot is (n - m). When rank $J(\theta)$ < m, the manipulability measure $\omega(\theta)$ becomes 0 and $d\theta$ can not be calculated from dX because of singularity. In this case, the robot loses some degrees of freedom, but the redundant robot uses the redundant degree of freedom to escape from this singularity status.

3-2. Singularity Status of the R-P System

The differential change of the end effector position is related with that of joint position by the Jacobian matrix. The Jacobian of the R-P system is as follows :

$$\begin{bmatrix} -r_{11}g_{11}+r_{21}g_{14} & -r_{11}r_{31}+r_{21}(r_{14}+a_6) & J_{11}s_5 & -J_{12}c_5 & J_{13}c_5 & -d_5c_5 & 0 \\ -r_{12}g_{12}+r_{22}g_{14} & -r_{12}r_{32}+r_{22}(r_{14}+a_6) & J_{11}c_5 & J_{12}s_5 & J_{13}s_5 & d_5s_5 & 0 \\ -r_{13}g_{13}+r_{23}g_{14} & -r_{13}r_{33}+r_{23}(r_{14}+a_6) & 0 & -a_4s_{56}+a_5c_6+a_6 & a_5c_6+a_6 & a_6 & 0 \\ s_6r_{11}+c_6r_{21} & -r_{31} & r_{31} & -s_5 & -s_5 & -s_5 & 0 \\ s_6r_{12}+c_6r_{22} & -r_{32} & r_{32} & -c_5 & -c_5 & -c_5 & 0 \\ s_6r_{13}+c_6r_{23} & -r_{33} & r_{33} & 0 & 0 & 0 & 1 \end{bmatrix}$$

$J_{11}=-r_{14}/c_5 \quad J_{12}=J_{11}-a_4c_{56} \quad J_{13}=d_5-a_4s_5$ (25)

$g_{11}=c_6r_{11}-s_6r_{21} \quad g_{12}=c_6r_{12}-s_6r_{22} \quad g_{13}=c_6r_{13}-s_6r_{23} \quad g_{14}=c_6r_{14}-s_6r_{24}+a_4c_5$

As the manipulability measure of the R-P system is not easy to evaluate because of 7 joints, the singularity position of the system can be investigated in view of the rank of the Jacobian matrix.

The Jacobian matrix of 5-degree robot is composed of 5 columns from the 3rd column to the 7th column in Eq.(25).

state 1)

$$s_{456}=0, \quad J_{11}=0$$
$$\theta_4+\theta_5+\theta_6=0^\circ, \quad a_6+a_5c_6-a_4s_{56}=0 \qquad (26)$$

In this case, the 3rd column and 7th column become equal which makes robot be in singularity status. When the robot becomes one kinematic model with the positioner, the Jacobian matrix is composed of 7 columns.

state 2)

$$S_{456}=0, \quad s_2=0, \quad s_3=0 \qquad (27)$$

In this case, the 4th and 5th row of the Jacobian matrix become dependent, which makes the robot be in singularity status.

state 3)

$$s_{456}=s_2, \quad s_3=0,$$
$$[c_2(r_{14}+a_2)-s_2r_{34}]=0 \qquad (28)$$

In this case, the 1st and 7th column of the Jacobian matrix become equal, which makes the robot be in singularity status.

3-3. The Distribution of Manupulability Measure in the Working Space

The manipulability of a robot is evaluated by manipulability measure and its distribution shows the overall structural properties of the robot. Therefore the manipulability measure can be used in the design and control of a robot, which makes the calculation and graphic method of the manipulability measure essential. But it is difficult to show the distribution of the manipulability measure in the whole working space since the Jacobian matrix in general is rank of 6. Because of this, let some degrees of freedom in working space or joint space be fixed. By the calculation of manipulability measure and its contour graph in a given section of the working space, we develop a method to visualize it.

The section of the working space is defined as the plane where one degree of freedom in X, Y and Z coordinates is fixed in working space. On this working plane the manipulability of a robot is calculated by fixing the orientation of the robot end effector.

The joint angle vector of n-degree of freedom robot is as follows :

$$\theta=[\theta_1, \ \theta_2, \ \cdots\cdots, \ \theta_n]^T \qquad (29)$$

The working space coordinate is represented as the position and the orientation and coordinates are shown in Fig. 2. In working space coordinates the position and orientation vector is defined as follows :

$$X=[x, y, z, \alpha, \beta, \gamma]^T \qquad (30)$$

where X, Y and Z are the position vector with with respect to the reference coordinate and α, β and γ are the Euler angles. Based on the above definitions, the visualization method of the contour for the distribution of manipulability in the working space is explained as a flow chart in Fig. 3.

After the section of the working space is decided, the positions are partitioned properly for investigation. At each partitioned positions, the Jacobian matrix is calculated by the inverse kinematic solution. Then the manipulability measure is found as in Eq.(23) and (24). A contour is drawn by connecting the equal values.

4. THE CONTROL OF MANIPULABILITY MEASURE IN A R-P SYSTEM BY REDUNDANT DEGERRS OF FREEDOM

In this section the possibility of the control method of the redundant degrees of freedom in R-P system is analyzed and the control method of the manipulability measure with redundant degrees of freedom is discussed.

The general solution of the linear algebraic equation in Eq.(21) is found as follows :

$$d\theta=J^*(\theta)dX+(I-J^*(\theta)J(\theta))dP \qquad (31)$$

where

$J(\theta)$	: pseudo-inverse transfomation of J
$I = n \times n$	: unit matrix
$(I-J(\theta)J(\theta)$	: projection operator
dP	: differential change of arbitrary vector

In this view point of maximizing the performance index, the redundant degrees are used to maximize the manipulability measure. In Eq.(31) $(I-J(\theta)\ J(\theta))dP$ which is used to maximize the performance index P represents the redundancy after the end effector accomplishes the main work.

The performance index P is defined as follows :

$$P = H(\theta) \qquad (32)$$

The performance index of the secondary work is defined as follows :

$$H(\theta) = K(\theta) \qquad (33)$$

The differential change of P is given as follows:

$$dP = \varepsilon K, \qquad \varepsilon = \partial H(\theta)/\partial\theta \qquad (34)$$

Here, K is chosen as follows not to exceed the maximum angular velocity of the each joint actuators.

$$K = (d\theta max - J(\theta)dx) \ / \ (I-J(\theta)J(\theta))\varepsilon \qquad (35)$$

The flow chart of the algorithm maximizing the performance index explained above is given in Fig. 4.

5. THE SIMULATION RESULTS AND DISCUSSIONS

5.1 The Distribution of the Manipulability Measure in Working Space

As the work is carried out on the positioner in the R-P system, the working space is confined on the positioner. The fixed degree of freedom in each cases are shown in Table 4. Fig.5 to Fig.8 show the distribution pattern of the manipulability measure in the cases of Table 4. In Fig.5(a) corresponding to case 1, the system is in singularity when the position of Y coordinate becomes 0 inch. This is the singular state 2) in Eq.(27). In Fig.5(b) corresponding to case 2, the X-Z work section is the contour map at the position of Y=0.

As shown in Fig.5(b), it is realized that every point in X - Z work section becomes singular as the manipulability measure is near zero in most cases.

The Fig. 6(a) corresponding to case 3 shows singularity point at X=Y=0. This is the singular state 3) in Eq.(28). Fig. 6(b) corresponding to case 4 which is the contour map the manipulability measure distribution on X - Z work section where the Y coordinate is zero in case 3. From Fig. 6(a) and Fig. 6(b) the robot and end effector are in vertical and on the Z axis of the reference coordinate.

Fig. 7(a) corresponding to case 5 shows that relatively larger manipulability measure is distributed on the whole positioner table.

Fig. 7(b) corresponding to case 6 shows the relatively small manipulability measure around X= -5 inch and Z= 3.5

inch without singularity points. Fig.8(a) corresponding to case 7 shows the similar pattern as the case 5.

But in Fig. 8(b), the contour of small manipulability measure has moved upward compared to case 6.

This happens as the tilting joint moves by -15°.

To represent the change of the manipulability measure due to the change of tilting joint and end effector motion, Fig. 9 shows the manipulability measure on the $\beta - \theta 2$ plane. Here the position is selected at a arbitrary point.

In Fig.9,as the tilting angle rotates positive from -90° and the end effector moves to the horizental position from vertical one, the manipulability measure increases.

5.2 Maximization of the Manipulability Measure in the Continuous Path Work

The algorithm for the manipulability measure maximization discussed in section 4 is applied to the R-P system and its applicability is discussed via 3 dimensional graphic simulation. The structure and joint vari-ables of the R-P system are shown in section 2 and its Jacobian is shown in section 3.2. The task is straight line trajectory following.

Example 1) Singularity avoidance in straight line following.

The R-P system operation is simulated to follow the straight line from the initial position Xi=[4 inch,4 inch, 2 inch, 0°, 0°,0°] to final position Xf=[4 inch, -4 inch, 2 inch, 0° ,0° ,0°]. The initial tilting angle is 0°.

Fig. 10 shows the manipulability measure along the straight line following. Here, the solid line is by the algorithm for the manipulability measure maximization and dashed line is by the case of dP = 0 in Eq. (31).

When the algorithm for the manipulability measure maximization is used, not only the desired position and orientation are possible in the case of singularity, but also singularity avoidance is considered. Therefore the whole operation is done better. Fig. 11 shows the simulation results by graphic simulator. Fig. 11(a) shows singularity when controlled dP = 0, the third joint passes slow 0°, but Fig. 11(b) shows which results are singularity avoidance by manipulability measure maximization.

Example 2) The manipulability measure mximization by the tilting joint motion of the positioner.

The R-P system follows the straight line from Xi=[4 inch, 4 inch, 2 inch, 0°, -45°, 0°] to Xf = [4 inch, -4 inch, 2 inch, 0°, -45°, 0°]. The initial tilting angle is -45°. Fig. 12 shows the trajectory of the manipulability measure in simulation.

During the operation the manipulability measure increases. The graphic simulation results in Fig. 13 show that the tilting angle of the positioner moves toward positive direction.

6. CONCLUSIONS

The kinematic analysis of a robot positioner system, existing 5 - degree robot and 2 - degree positioner,as a way to increase the robot performance results the followings :

1) The inverse kinematic solution of the robot positioner system was found.
2) By the contour of the performance index, the orientation of the robot end effector and the positioner tilting joint was investigated to increase the manipulability measure of the robot-positioner system.
3) By the redundancy control of the robot - positioner system, the whole operation in the presence of singularity was sucesful and a numerical example was given.

In the future, the visualization method such as a contour graph can be applied to the computer aided design of a robot system. For the analysis of the manipulability in 3-dimensional working space, the 3-dimen-sional graph of the manipulability measure is necessary. Also, the manipulability should be considered in the design of a positioner.

REFERENCES

1. Khosla,P.K. et al, 1986, "An Algorithm for Seam Tracking Application", The International Journal of Robotics, Vol.3, pp.27-41
2. Jeon, E.S., et al, 1986, " Trajectory Control of Robot System by One Kinematic Modeling", Proc. of KSME, pp. 47-51.
3. Yoshikawa, T., 1984, " Analysis and Control of Robotic Manipulators with Redundancy, " Robotics Research: The First Int. Symposium, ed. Brady, M. and Paul, R. P,pp. 735-748.
4. Uchiyama, M, et al, 1984, " Performance Evaluation of Manipulators using the Jacobian and Its Applications to Trajectory Planning", the 2nd Robotics Research, ed. Hanaffusa, H. et al, MIT Press, pp. 447-454.
5. Homsup, W. and Anderson, J.N., 1986, "Performance Evaluation of Robot Manipulators", IEEE, Proc. of American Control conference, Vol.1, pp. 130-1366. Paul, R.P., 1981, Robot Manipulator: Mathematics, Programming and Control, MIT Press.
7. Nakamura, k. and Hanafusa, H., 1984, " Task Priority Based Redundancy Control of Robot Manipulators", The 2nd Robotics Research, pp. 155-162.
8. Luh, J.Y.S. and Gu, Y.L., 1985, "International Robots with Seven Joints, " IEEE International Conference on Robotics and Automation, pp. 1010-1015.
9. Wang, L.T. and Ravani, B., 1985, "Recursive Computations of Kinematic and Dynamic Equations for Mechanical Manipulators", Vol. RA-1, No.3, pp. 124-131.
10. Liegeois, A., 1977, " Automatic Supervisory Control of the Configuration and Behavior of Multibody Mechanism" IEEE Trans. SMC-7, No.12, pp. 868-871.

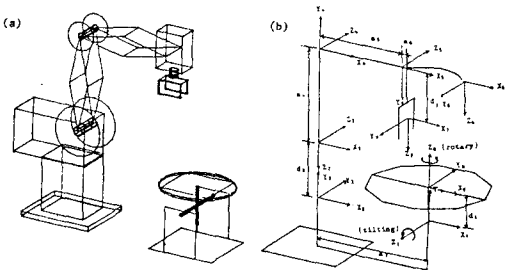

Fig. 1 A schemetic drawing of Rhino-XR3 and rotary-tilting carousel
(a) Configuration of R-P system.
(b) Coordinate system of R-P system)

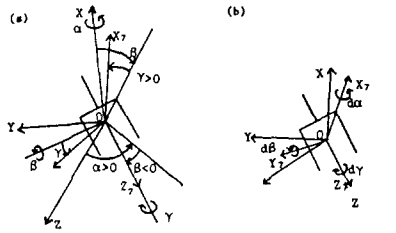

Fig. 2 Definition of the hand orientation angles and their differential change

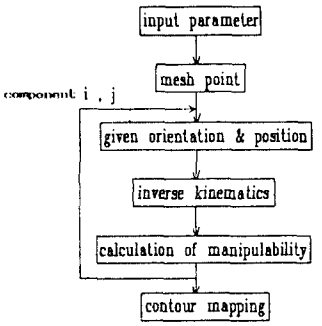

Fig. 3 Flow chart of the contour map for the distribution of manipulability

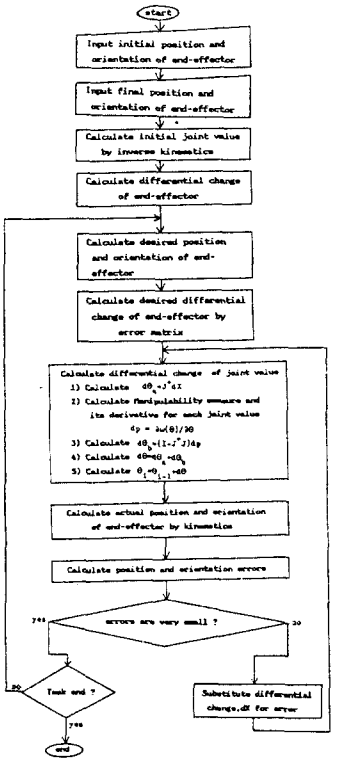

Fig. 4 Flow chart of the algorithm which maximize manipulability measure

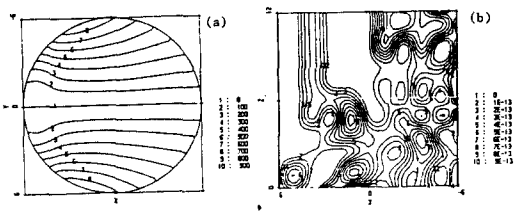

Fig. 5 Distribution of manipulability in the work space for Case 1,2

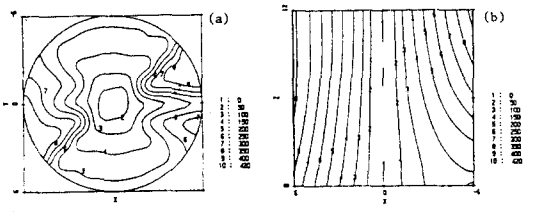

Fig. 6 Distribution of manipulability in the work space for Case 3,4

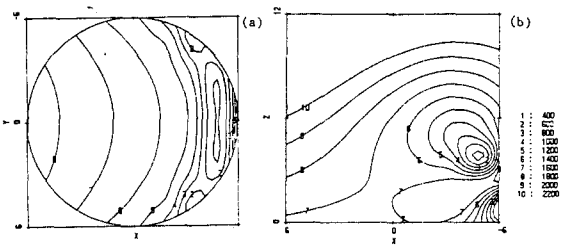

Fig. 7 Distribution of manipulability in the work space for Case 5,6

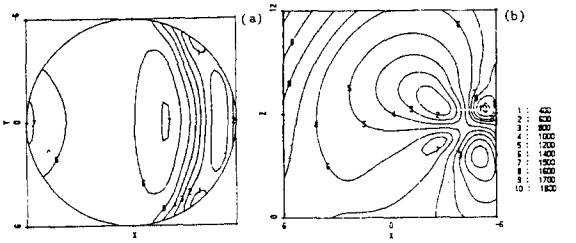

Fig. 8 Distribution of manipulability in the work space for Case 7,8

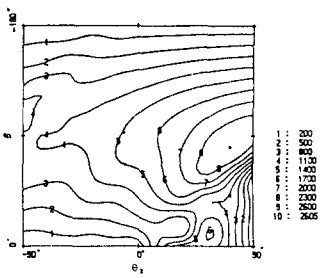

Fig. 9 Manipulability due to the change of tilting joint and end-effector motion

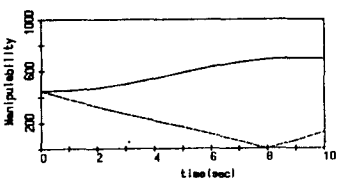

Fig. 10 Comparision of manipulability for straight line task
(…… : Control algorithm $dP=0$ in eq. (31)
…… : Control algorithm eq. (31) ~ (35))

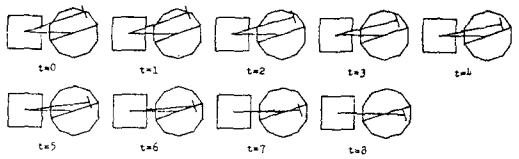

Fig. 11 3-D graphic simulation for straight line task

(a) Control algorithm : $dP=0$ in eq. (31)

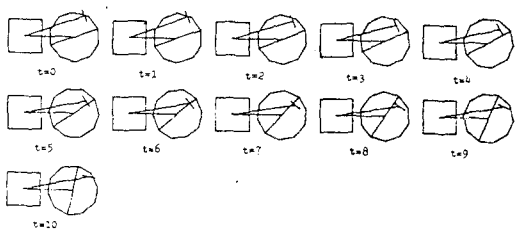

Fig. 11 (b) Control algorithm : eq. (31) ~ (35)

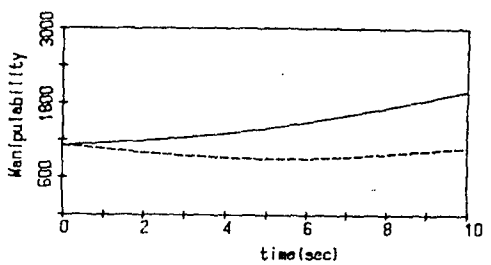

Fig. 12 Comparision of manipulability for straight line task with tilting motion
(····· : Control algorithm $dP=0$ in eq. (31)
—— : Control algorithm eq. (31) ~ (35))

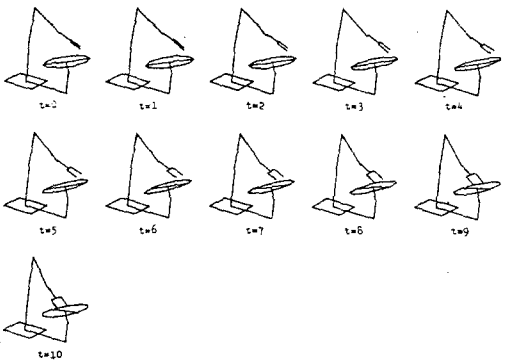

Fig. 13 3-D graphic simulation for straight line task with tilting motion
(a) Control algorithm : $dP=0$ in eq. (31)

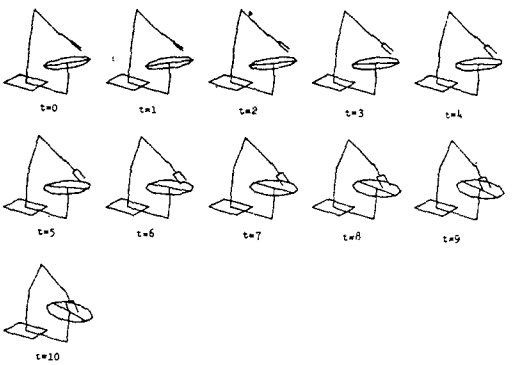

Fig. 13 (b) Control algorithm : eq. (31) ~ (35)